Hindawi
Journal of Nanomaterials
Volume 2022, Article ID 3767355, 10 pages
https://doi.org/10.1155/2022/3767355

Research Article

Plasma Deposition of Gallium Arsenide Nanoclusters on a Silicon Matrix

Kulpash Iskakova

Department of Physics and Mathematics, Abai Kazakh National Pedagogical University, Almaty, Dostyk 13, Kazakhstan

Correspondence should be addressed to Kulpash Iskakova; ahmanovakulpash@yahoo.com

Received 14 February 2022; Accepted 12 March 2022; Published 30 March 2022

Academic Editor: Mohammad Rahimi-Gorji

In the plasma state, a polar semiconductor gallium arsenide (GaAs) is deposited on a nonpolar silicon (Si) matrix in the <111> direction. Further qualitative and quantitative analyzes were carried out with the resulting GaAs/Si structure on a plasma-beam device. We have chosen the optimal characteristics of this pulsed method for the deposition of GaAs from a plasma onto silicon (Si) created by a powerful ion beam. The optimal modes of the effect of temperature, electric field, and interval of pulse action on GaAs/Si quantum-well heteronanostructures were considered. In the implementation of application of this structure in applied works related to opto- and nanoelectronics, active elements of solar cells require defect-free compositions with ideal geometric parameters. Based on these experiments, the optimal mode of plasma influence on the formation of nanoclusters on the surface of the irradiated sample was chosen. SEM, EDS, and X-ray diffraction analysis methods were used to determine such parameters as the structure, microhardness, phase and elemental composition of the irradiated Si silicon surface, as well as the penetration depth of GaAs deposited on a single-crystal matrix. This work presents an experimental implementation of preparation of a gallium arsenide nanolayer and an applied theoretical analysis of the GaAs/Si heteronanostructure. We deposited gallium arsenide compounds from the plasma state on the surface of a silica crystal and studied the resulting structure by physicochemical methods.

1. Introduction

The required characteristics of GaAs/Si structures in electronic elements, active elements of solar panels, and light-emitting devices are reduced owing to the presence of defects. To improve the properties of the structure of the direct-gap semiconductor GaAs on silicon, this experiment was carried out based on plasma irradiation. In plasma-beam irradiation, places in the Si sublattice of silicon can be occupied by Ga or As, and, depending on this, silicon can be a donor or acceptor. The low-defect GaAs/Si nanostructure thus obtained is an important object for improving the photoelectric and optical properties of this matrix.

The purpose of this article is to describe the corresponding mechanisms of the gallium arsenide nanofilm formation on a silicon matrix using the developed method of plasma deposition. The following case of the possibility of conducting an experiment using a low-temperature gas plasma (LGP) for heterogeneous physical and chemical processing processes at the gas (gas plasma)-solid body interface has been chosen. LGP is a conducting medium, a source of particles participating in the process, and a process activator at the same time. We determined the conditions under which almost defect-free GaAs nanofilms 50-70 nm in size are formed.

The experimental part of the work on deposition of gallium arsenide on silicon in a plasma-beam discharge was carried out using a plasma-beam installation (PBI). The main elements of the PBI are an electron beam cannon (EBC), plasma-beam discharge (PBD) chamber, EBC pumping chamber, interaction chamber, electromagnetic coils, target device, sluice device, and loading chamber.

Gallium arsenide (GaAs) is deposited on a silicon (Si) matrix in a plasma-beam discharge. A special collector unit for plasma-beam installation was developed, and the operating modes of the plasma-beam installation, in which gallium arsenide was deposited on a silicon substrate, were determined.

GaAs (100) layers were used to study the surface structure of gallium arsenide on a silicon matrix. The surface state

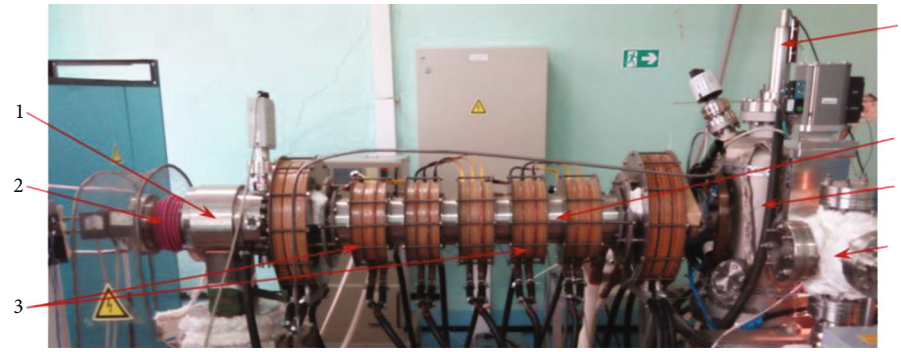

Figure 1: General view of the plasma-beam installation. (1) Electron beam cannon chamber; (2) electron beam cannon; (3) electromagnetic system; (4) Langmuir probe; (5) plasma-beam discharge chamber; (6) interaction chamber; (7) loading chamber.

of the GaAs layer was studied using a scanning microscope and energy dispersive spectral analysis (EDS). To obtain a mass flow (sputtering) of GaAs uniform in composition and to remove the oxide film from the target surface, preliminary sputtering was carried out for 3 minutes. The phase composition of GaAs on the matrix was determined using X-ray diffraction analysis, the results of which are shown in the X-ray diffraction patterns of the samples. The analysis of the SEM image of the surface relief was carried out using a program that allows tracing the image of the surface relief. The structure of the thin surface region of the samples was studied by high-energy electron diffraction.

2. Materials and Methods

Gallium arsenide has better semiconductor characteristics than silicon. The electron mobility of GaAs is to 5-6 times higher than that of Si. These and other properties of GaAs determine its higher frequency and power-consuming characteristics [1–4].

Previously, we investigated the structures of empty and filled cells of III–V nanoparticles using first-principles calculations. Our results show that in the range of small sizes, in accordance with the characteristics of their valence bonds, it is easy to understand the available stability. The gallium atom has only one $4p$ electron, and on the atomic orbitals of the arsenic atom there are three $4p$ electrons. Thus, the Ga atom in the cluster will have fewer bonds than the As atom. When they form mixed clusters, the Ga atoms become atoms of the faces, which require fewer bonds. All of them have filled cell structures, which we reported for III-V nanoparticles [5–8]. The obtained values of the discontinuities in the uniform increase and amplitude of the electronic densities ρ $(Cu_2O)_n$ [9, 10] in comparison with Ga_mAs_n show that the interspaces are features of the material, and the nature of such bonds plays an important role. Therefore, nanoparticles of Ga_mAs_n while increasing in size produce three-dimensional structures faster in comparison with the structure $(Cu_2O)_n$ [11].

The experimental work on the deposition of GaAs on Si was carried out on a PBI using plasma-beam discharge. The main elements of the PBI are an electron beam cannon (EBC), plasma-beam discharge (PBD) chamber, EBG pumping chamber, interaction chamber, electromagnetic coils, target device, sluice device, and sample loading chamber. A general view of the PBI is shown in Figure 1.

The PBI provides the following parameters of the plasma flow:

(i) Diameter of the plasma stream in front of the target up to 30 mm

(ii) Intensity of the magnetic field created on the axis of the camera PBD 0.1 T

(iii) Maximum current in the plasma is 1 A

(iv) Plasma density in the beam up to 10^{18} m^{-3}.

The electronic temperature of the plasma was 5-15 eV.

The operation principle of the installation is as follows. The electron gun generates an axially symmetric electron beam. The cathode of the cannon was heated via electron bombardment from the filament. The power of the gun was controlled by the power of the cathode heating and the accelerating voltage of the electron beam. Autonomous pumping of the gun provides a vacuum drop between the gun and discharge chamber. The electron beam interacted with the working gas in the discharge chamber, forming a plasma filament. The electromagnetic system, which consists of coils, creates a longitudinal magnetic field in the discharge chamber. The geometric parameters of the plasma beam were controlled using an electromagnetic system [12].

To fix the Si substrate, it is necessary to develop a separate collector assembly that can be installed in the PBI interaction chamber. The heater was integrated into the manifold assembly to maintain the desired substrate temperature. All parts of the manifold assembly were made in accordance with the requirements for ensuring vacuum.

The expected temperature of the Si substrate in the experiments is $t_{Si} = 1100°C$. During the experiments, the temperature of the GaAs sample (t_{GaAs} 600°C, 700°C, and 800°C) and the energy of Ar ions (E_{Si} 150 eV, 1000 eV, and 1500 eV) were varied. Changing the GaAs temperature is achieved by controlling the EBC power and the value of the ion energy by changing the negative potential applied to the Si substrate. Sputtering of GaAs was carried out in plasma-beam discharge mode using an

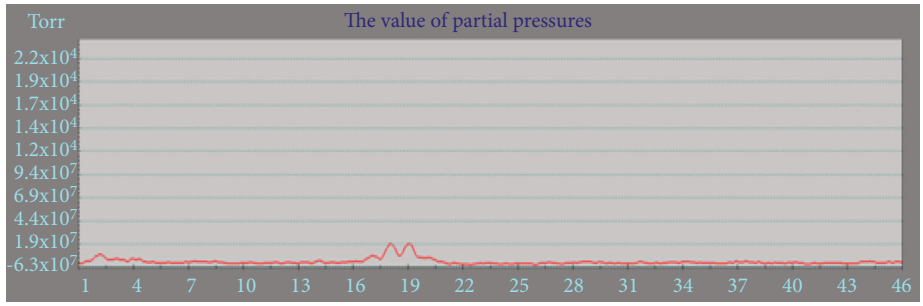

Figure 2: Graph of partial pressures of residual gases when testing manifold assemblies.

argon (Ar) working gas. To obtain a uniform compositional mass flow (sputtering) of GaAs and remove the oxide film from the surface, it was necessary to carry out preliminary sputtering for 3 min.

To ensure the effective deposition, the distance between the GaAs plane and the Si substrate should be 7–12 cm. The angle of incidence of the argon ion flux relative to the normal to the plane of the GaAs sample ranged from 30° to 60°.

To carry out experiments on the deposition of GaAs on a Si substrate, parts of the PPU collector unit were specially made. The assembly and installation of the collector unit on the PPU interaction chamber was carried out. On the chamber, the internal cavities of the installation were evacuated to a pressure value of $1 \bullet 10^{-7}$ Torr with a leak test. The heating element was degassed to a temperature of 1200°C; the temperature was measured by the pyrometric method. The values of current and voltage supplied to the heating element were recorded periodically. A high voltage of up to 1500 V is applied to the GaAs sample holder for sputtering. It is necessary to ensure the location of the silicon substrate relative to the normal of the collector assembly at an angle of 45° and to make it possible to heat the silicon substrate to 1200°C. Prepare the working gas-Ar with preliminary evacuation of the gas purge system so that no other gases are present. The Si temperature should be controlled by the pyrometric method from the front side and the GaAs target by a thermocouple from the back side. Then, determine the optimal operating modes of the FPU, in which the deposition of GaAs on Si will occur. During the experimental work, the plasma parameters are determined by the method of probe diagnostics. After the experiments on the deposition of GaAs, X-ray phase (X-ray) analysis of the Si surface was carried out. For quantitative and qualitative analysis, microstructural (SEM) and elemental (EDS) analysis of the surface of the silicon substrate was carried out.

The working chambers of the installation chambers were evacuated using turbomolecular pumps TMU-262, TMU-521, and a Varian SH-110 backing pump. The pressure in the EBC pumping chamber was measured using a Pfeiffer IMR-265 pressure sensor in the PPR chamber and a Pfeiffer PBR-260 pressure sensor in the interaction chamber using a Pfeiffer PKR 261 pressure sensor. Pressure monitoring in the cavities of all chambers and management of turbomolecular and prevacuum pumps were carried out using the Combi-Gauge controller. To check the tightness of the collector

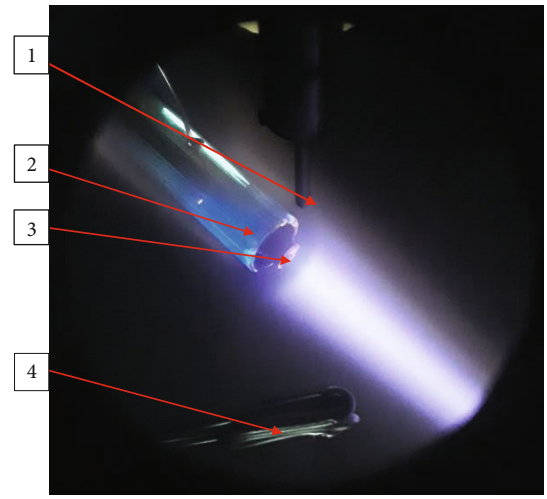

Figure 3: Snapshot during the experiment. (1) Langmuir probe; (2) main collector; (3) GaAs; (4) additional collector with Si.

unit, the partial pressures of the residual gases in the interaction chamber were recorded using a CIS-100 quadrupole mass spectrometer with its own vacuum pumping system. The pressure and flow rate of water in the cooling system were measured by pressure sensors Metran-55DA and flow meters VST-15 in the inlet manifold path and amounted to 0.25 MPa and 0.06 kg/s, respectively. To carry out degassing of the heating element, a laboratory autotransformer from Resanta TR/5 with a power of 5 kW was used. The temperature of the heating element was measured using a LumaSense ISR6 pyrometer with a measurement range of 800–2550°C. The control of the bench automation units was carried out in manual mode. The temperature of the front side Si was measured using a Metis M322 two-color pyrometer with a measurement range from 500°C to 1800°C. The temperature of the rear side of the GaAs target was measured using an XA-type thermocouple. The collector assembly of the GaAs target was galvanically isolated from the potential supply unit during testing. Recording of current information on a magnetic medium and displaying it on the display screen was performed using the information-measuring system PBI.

2.1. Testing and Experimental Work. An ultrahigh vacuum was carried out on the PPU chamber for argon plasma,

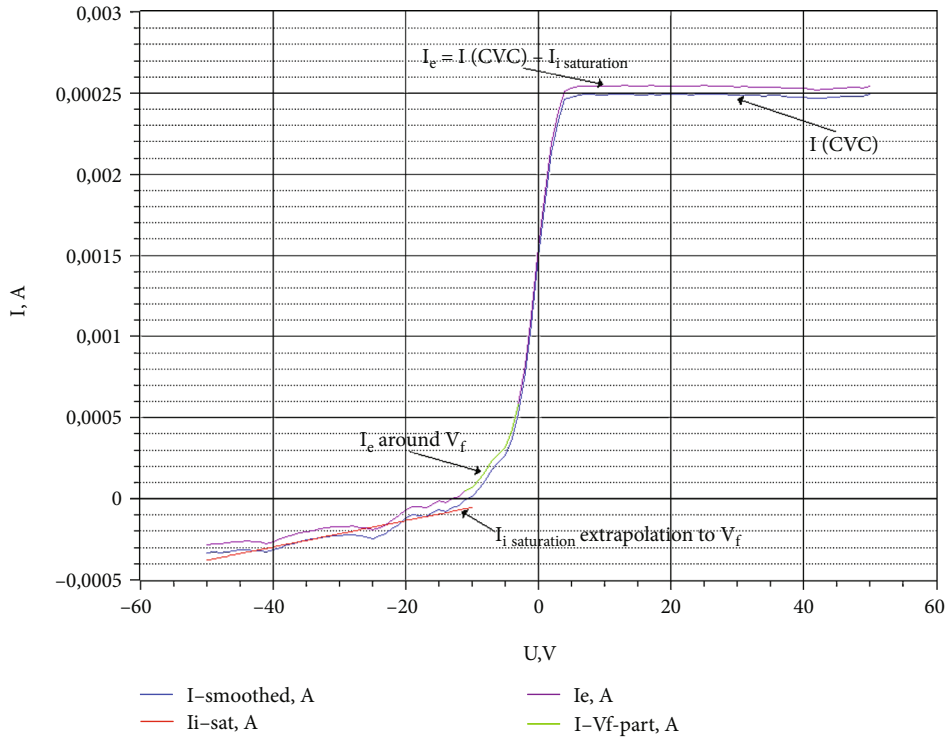

Figure 4: Experimental I-V characteristic of the PBI plasma during the deposition of GaAs on Si.

Table 1: Deposition modes.

Sample number	Deposition time, hour	Argon ion energy, eV	Silicon temperature, ˚C	GaAs temperature, ˚C
1 (27-60-500)	1	500	27	300
2 (27-90-500)	1.5	500	27	300
3 (27-120-500)	2	500	27	300
4 (27-150-500)	2.5	500	27	300
5 (27-60-1000)	1	1000	27	300

where the silicon matrix and the gallium arsenide sample are located. The value of pressure during evacuation in the path of the foreline pumps was $1.7 \bullet 10^{-2}$ Torr, and in the high-vacuum chambers of the installation, it was $1 \bullet 10^{-7}$ Torr. In the collector assembly during testing, the partial pressures of the residual gases amounted to the limit value for the deposition of gallium arsenide. The value of partial pressures of residual gases during evacuation is shown in Figure 2.

According to the results of our observations, it was found that the main peaks of partial pressure with a value of $\sim 1.9 \bullet 10^{-7}$ Torr are water vapor. The value of the partial pressures of the remaining gases are at the background level, which indicates the complete sealing of the connections of the collector assembly [13, 14]. The voltage was applied to the collector unit in steps from 0 V to 1500 V with a step of 100 V. During the experiment, no breakdowns were recorded when the voltage was applied. In view of the design features of the PPU and the experimental conditions, silicon samples were prepared in the form of a rectangular parallelepiped with dimensions of $25 \times 25 \times 5$ mm.

As a result of repeated test work to determine the optimal modes of deposition of GaAs on Si, we found that deposition occurs at a GaAs target temperature of 300 ± 10°C, an ion energy of 500 eV, 1000 eV, and Si temperature 27°C in the SPR mode using argon working gas. The duration of plasma-beam exposure to GaAs was as follows: 1 hour, 1.5 hours, 2 hours, and 2.5 hours. To obtain a mass flow (sputtering) of GaAs uniform in composition and to remove the oxide film from the target surface, preliminary sputtering was carried out for 3 minutes. The consequences of the action of argon plasma on gallium arsenide and its sputtering in the form of a light beam are shown in Figure 3, where a silicon matrix is located at an angle of 45 to the normal of the collector node. The picture was taken during the experimental work on the plasma deposition of GaAs.

Qualitative measurements of the plasma density were carried out in the ion saturation mode. For a quantitative assessment of the local parameters of the plasma, its current-voltage characteristics (CVC) were measured, which are shown in Figure 4 for a given value of the accelerating voltage.

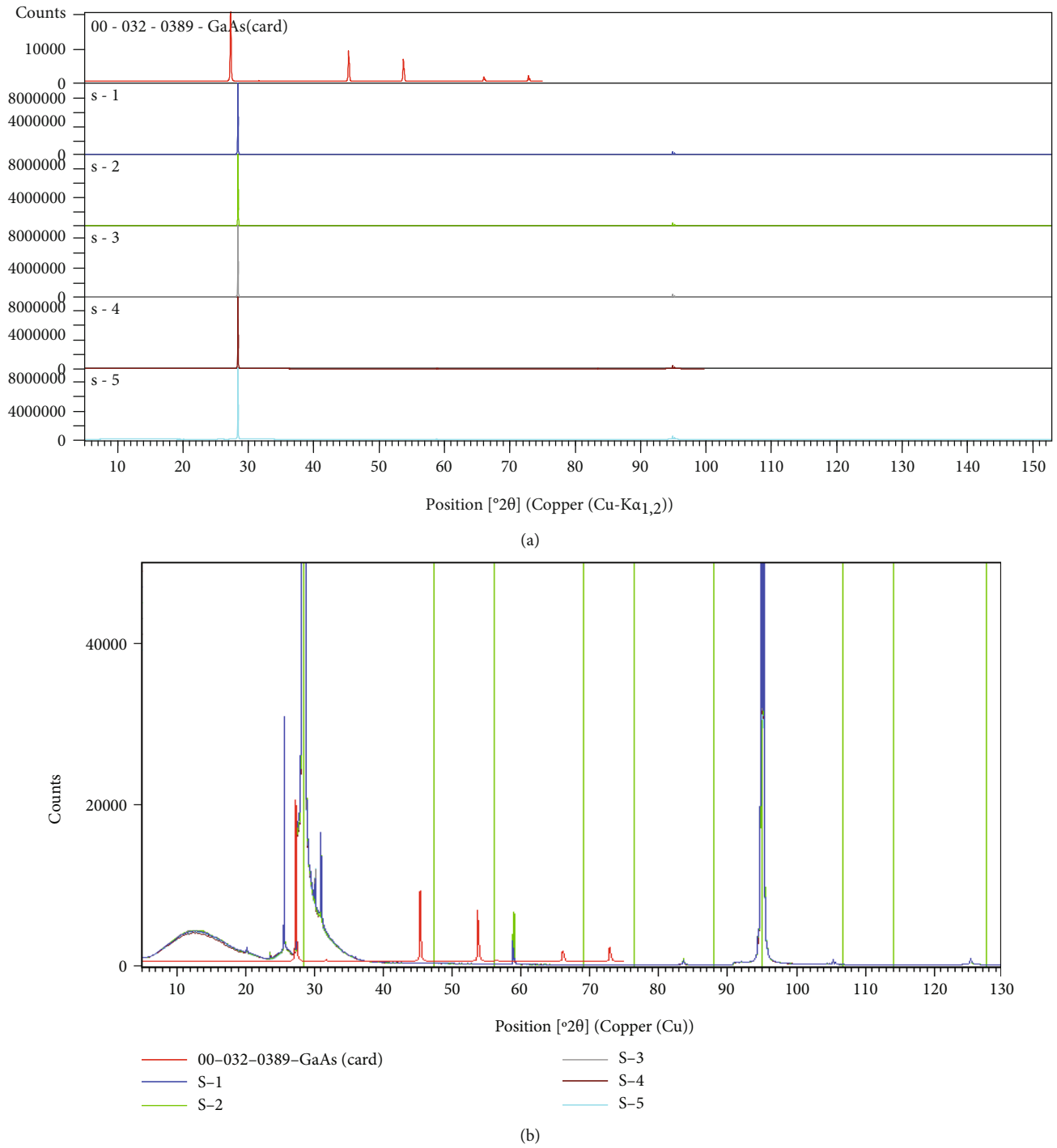

FIGURE 5: General view of diffraction patterns of samples after experiments after deposition of GaAs on a single-crystal Si substrate: (a) comparative diagram of diffraction patterns; (b) an enlarged fragment along the ordinate axis (from 0 to 50 thousand imp.) and overlaying a silicon bar diagram.

The local parameters of the argon plasma beam are as follows: electron temperature $T_e = 3.9 \bullet 10^4 K$ and plasma ion concentration $n_i = 2.8 \bullet 10^{17} м^{-3}$. Based on the results of the test work, the choice of optimal deposition modes was made, which are characterized by the parameters given in Table 1. Five experiments on the deposition of GaAs on Si samples were carried out, respectively, in these selected modes.

3. Results of X-Ray Phase Analysis after Experiments

The composition of the nanolayer of the GaAs compound on the Si matrix was determined by X-ray diffraction analysis on single crystals extracted from the sample. The diffraction patterns of the samples were recorded on an Empyrean

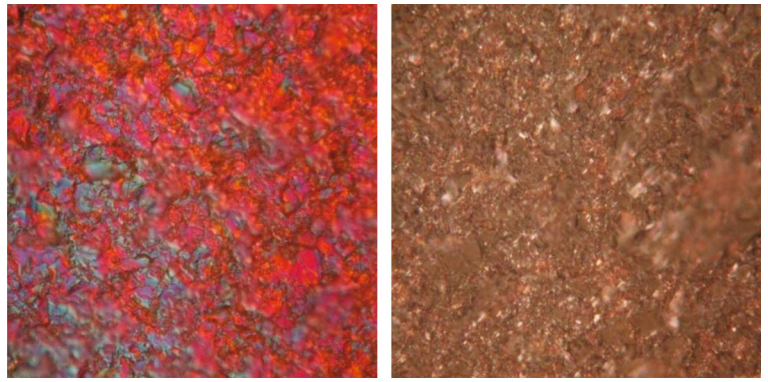

(a) (b)

Figure 6: The surface of the original Si (×1000): (a) the image obtained using the DIC module and (b) the image obtained in a light field.

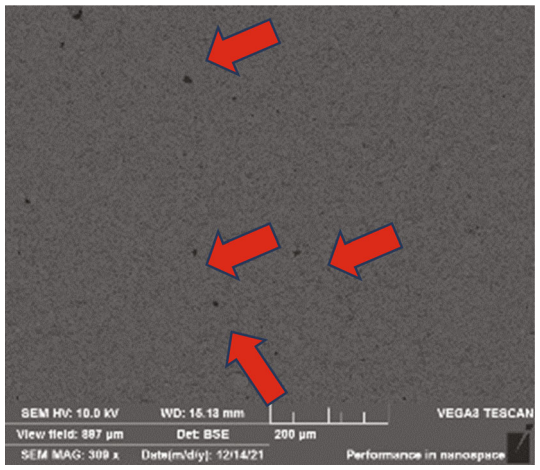

Figure 7: Snapshot of the Si surface with a deposition time of more than 120 minutes.

diffractometer in the PIXcel1D detector mode. The purpose of X-ray phase analysis was to determine the phase composition of the surface of Si samples after GaAs deposition. The exposure time (time per step) during filming was 30.6 s, the scanning step size for diffractograms was –0.013°2θ, the investigated angular range was –5-153°2θ. To identify the phase composition, the Crystallography Open Database (hereafter referred to as COD [15]) and PDF-2 ICDD Release 2004 database were used [16]. During the deposition of GaAs on Si, we determined that its phase composition can be detected only at small angles of the studied angular range and provided that it is located at a depth of up to 38 μm with a diffractometer. Graphs of Figures 5(a) and 5(b) will show comparative diagrams of diffraction patterns and an enlarged fragment along the ordinate axis (from 0 to 50 thousand pulses). Figure 5(a) shows the appearance of the diffraction patterns of GaAs (in red) and five experimental samples deposited with a nanolayer on silicon. It can be seen from the diffraction pattern that the maximum phase composition for standard GaAs is located at the angle of 27°2θ. This peak for GaAs nanolayers in all GaAs/Si samples is shifted by an angle of 28.5°2θ. In Figure 5(b), a bar diagram of crystalline Si (cubic syngony, space group Fd-3 m, lattice parameter 5.430 Å) is added to the studied diffraction patterns, which is available in the diffraction data base used for analysis. The bar graph of Si is marked in green.

Table 2: Elemental composition of gallium arsenide on the Si matrix by deposition modes.

Elemental composition by modes			
Mode 27-60-500			
	Ga	As	Sum
At. %	55.44	38.11	100.00
Mass%	51.86	33.18	100.00
Mode 27-90-500			
At. %	58.64	41.36	100.00
Mass%	60.37	39.63	100.00
Mode 27-120-500			
At. %	59.20	40.80	100.00
Mass%	60.93	39.07	100.00
Mode 27-150-500			
At. %	57.77	42.23	100.00
Mass%	59.51	40.49	100.00
Mode 27-60-1000			
At. %	57.18	42.82	100.00
Mass%	58.93	41.07	100.00

The basis of the phase composition of the samples is single-crystal Si, which is confirmed by the coincidence of the peaks in the diffraction patterns with the line diagram of the Si card. Very high intensity levels are noted in the diffraction patterns obtained from single crystal Si. It is known from the research results that the level of intensity of the maximum peak of GaAs is 400 times less than the intensity of single-crystal Si. This is the main reason for the difficulty in identifying GaAs peaks. In this regard, it is advisable to conduct a study with a scanning electron microscope (SEM) and analyze the energy dispersive spectrum (EDS).

4. Results of SEM and EDS Analyses

To analyze the relief of the GaAs surface, we used a two-dimensional image of its section obtained with a scanning

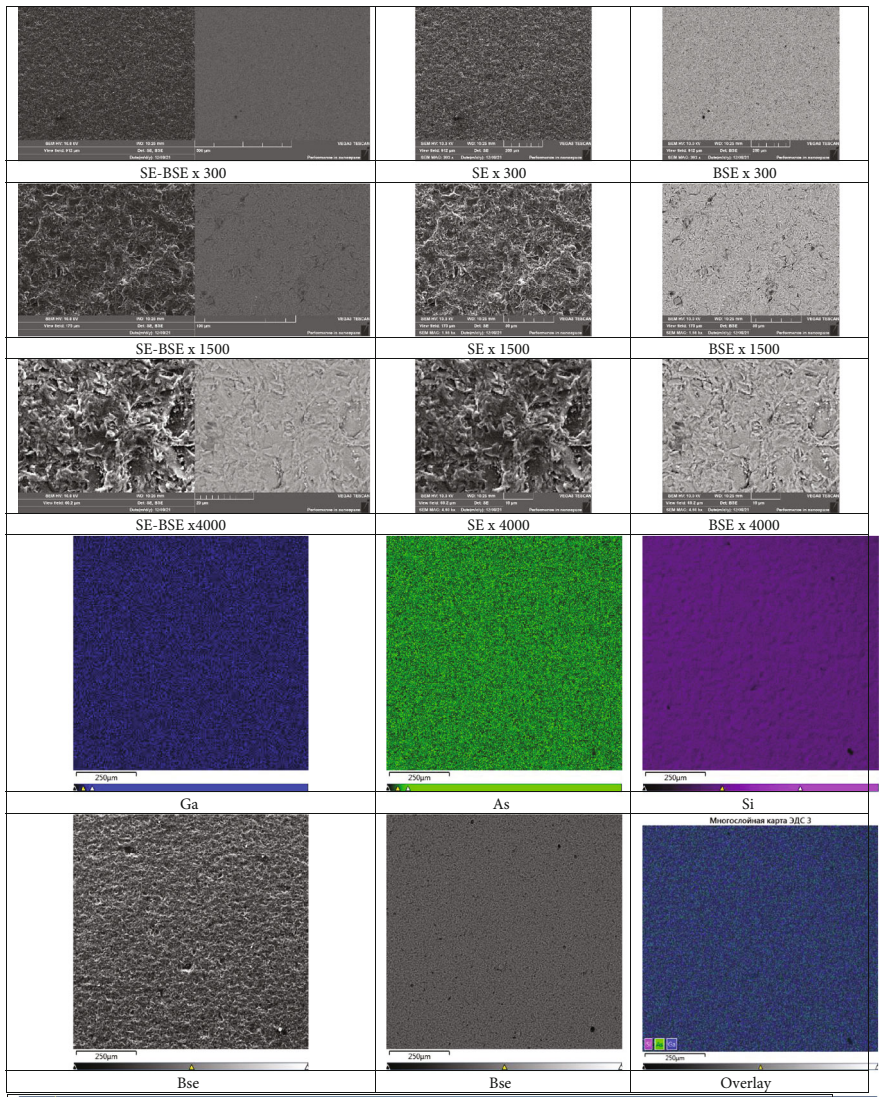

Elemental composition				
Spectrum name	Si	Ga	As	Sum
Mass %	6.44	55.44	38.11	100.00
Spectrum name	Si	Ga	As	Sum
At. %	14.96	51.86	33.18	100.00

(a)

Figure 8: Continued.

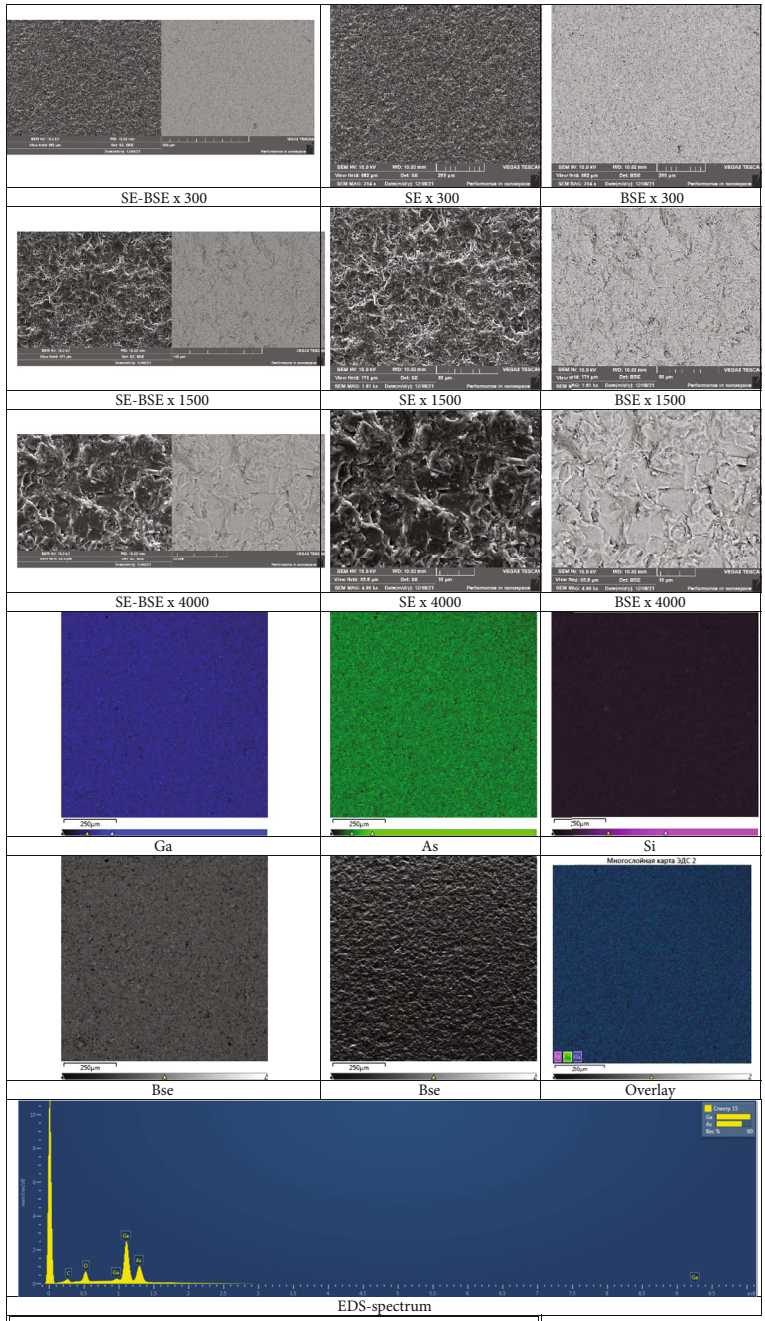

Elemental analysis			
Spectrum name	Ga	As	Sum
Mass %	57.18	42.82	100.00
Spectrum name	Ga	As	Sum
At. %	58.93	41.07	100.00

(b)

Figure 8: SEM images and the results of the elemental composition of the Si surface after GaAs deposition, depending on the experimental conditions. (a) SEM images of the morphology and elemental composition of sample 1 (27-60-500) (temperature Si: 27°C; duration of exposure: 60 minutes; energy of argon ions: 500 eV). (b) SEM images of the morphology and elemental composition of sample 5 (27-60-1000) (temperature Si: 27°C; duration of exposure: 60 minutes; energy of argon ions: 1000 eV).

electron microscope. Quantitative studies of the surface are confirmed by the obtained results of the EDS spectra and the relative mass and molar ratios according to this analysis. For all five obtained samples, the states of the surfaces of the GaAs layer were studied using a scanning microscope and energy dispersive spectral analysis (EDS) to determine the quantitative composition. According to the results of the microstructural studies, the surface of the original Si (×1000): on the left, obtained using the DIC module; on the right, an image obtained in a bright field. The

microstructural image of the surface of the original Si (see Figure 6) is characterized by a developed morphology and has a coral-like relief, with a large number of sharp edges on protrusions and depressions. Pores or cracks were not detected on the surface.

SEM images and the results of the elemental composition of the Si surface after GaAs deposition, depending on the experimental conditions, show how the surface profile and nanolayer concentration change. In SEM-EDS analysis, the depth of X-ray radiation generation is determined by the depth of penetration of the probe electron beam into the sample, which depends on the energy of the primary electrons and the density of the material under study [17, 18]. According to the results obtained, the thickness of the GaAs layer increased with an increase in the ion energy. Quantitative studies of the surface are confirmed by the obtained results of the EDS spectra and the relative mass and molar ratios according to this analysis. For all five obtained samples, the states of the surfaces of the GaAs layer were studied using a scanning microscope and energy dispersive spectral analysis (EDS) to determine the quantitative composition. This is confirmed by the results of elemental analysis. An increase in the duration of the deposition process also leads to an increase in the thickness of the GaAs layer. However, it should be noted that with a process duration of 120 min or longer, the Si surface is characterized by a more developed morphology, and additional particles are observed, which are most likely artifacts of carbon deposits (marked with red arrows in Figure 7), and their number increases with an increase in the duration of deposition [19–25]. Table 2 presents the results of determining the composition of phases in the GaAs/Si systems by the energy dispersive analysis method using the INCAEnergy detector [26, 27].

With a further increase in the duration of exposure and the energy of argon ions during the deposition of GaAs, the surface of the samples does not undergo significant changes. The surface morphology after GaAs deposition is smoothed out, and the depressions and protrusions of the faces become less pronounced and have a "melted" appearance. It can be seen from the SEM image (Figures 8(a) and 8(b)) that the profiles do not change significantly with respect to changes in the temperatures, deposition time, and ion energy of the argon plasma beam. These figures show nanolayers obtained in two selected modes. Provided that the temperature of Si is 27° C, exposure time 60 minutes, and the energy of argon ions is 500 eV, for these parameters, atomic concentrations for Ga 55.44 and As 38.11 were obtained from the EMF analysis for these parameters, and the weight concentrations are 51.861:33.18, respectively; the image profiles are shown in the figure in Figure 8(a). With an increase in the energy of argon ions to 1000 eV, the Si temperature and exposure time took on the values of the above state. In this case, the thickness of the GaAs layer increases, and the atomic concentrations for Ga are 57.18 and As, 42.82, and the weight concentrations correspond to 58.93: 41.07 for Ga : As. The image profiles are shown in Figure 8(b).

Studies performed using energy dispersive spectral analysis (EDS) for five samples obtained at different mode parameters showed that the relative atomic and weight ratios of arsenide to gallium change by 0.02%. In order to improve the accuracy of determining the composition of phases by the method of energy dispersive microanalysis, standardization was carried out using a specially prepared standard based on a GaAs compound. Table 2 presents the results of determining the composition of phases in the GaAs/Si systems by the energy dispersive analysis method using the INCAEnergy detector. The result of processing by methods of mathematical statistics for determining the atomic and weight concentrations of elements is no more than 0.1%.

As a result of linear analysis and mapping, it was revealed that the deposited GaAs layer has a uniform distribution over the entire Si surface, and the ratio of its elements varies depending on the deposition mode and conditions. Thus, the growth of the gallium arsenide film occurs with the preservation of its structure in all the states chosen by us in the first four states, where the exposure duration increases and the Ga : As ratios in atomic concentrations decrease from 1.45 to 1.36 and the weight concentrations from 1.56 to 1.46. The difference in the concentration ratio of Ga to As decreases. At different plasma energies, 500 eV and 1000 eV, and at the same exposure time of 60 minutes, the ratio of atomic concentrations of Ga to As is 1.45: 1.33; the weight concentrations decrease from 1.56 to 1.43. As the plasma energy increases, the concentration ratio of Ga to As decreases. At the same time, it should be noted that, according to the obtained data of energy dispersive analysis, there are no foreign elements in the selected regimes of GaAs deposition on Si.

5. Conclusion

GaAs (100) nanolayers were obtained using the plasma deposition method under the optimal conditions chosen by us. The study of these nanolayers with a scanning electron microscope shows the formation of densely adjoining nanoclusters of layers consisting of GaAs in ratios approximately equal to 1:1.3. It has been established that with an increase in the duration of exposure and ion energy, an increase in the thickness of the GaAs layer is observed. In this case, an increase in the duration of the deposition process to more than 120 minutes leads to a change in the morphology of the silicon surface with the deposited layer. According to the results of linear analysis and mapping, it was found that the deposited GaAs layer has a uniform distribution over the entire Si surface and the ratio of its elements varies within 0.05%, regardless of the modes and conditions of deposition.

Data Availability

The date of table, the grafical data used to support the findings of this study are included within the article.

Additional Points

The results presented clearly, honestly, and without fabrication, falsification, or inappropriate data manipulation (including image-based manipulation). The authors adhered to discipline-specific rules for acquiring, selecting, and processing data. All data are available in the main text.

Conflicts of Interest

The authors have no relevant financial or nonfinancial interests to disclose.

Authors' Contributions

KI was assigned in the conceptualization; methodology; investigations; visualization; funding acquisition; supervision; writing, original draft; and writing, review and editing. SJE, MJM, JLS, and EH were assigned in the project administration.

References

[1] S. Makram-Ebeid, P. Langlade, and G. M. Martin, *Proceeding of the Third Conference on Semi-Insulating III-V Materials*, D. C. Look and J. S. Blakemoore, Eds., Shiva, Nantwich, Nantwich, England, 1985.

[2] A. Kokaji, "XCrySDen—a new program for displaying crystalline structures and electron densities," *Journal of Molecular Graphics & Modelling*, vol. 17, no. 3-4, pp. 176–179, 1999.

[3] I. L. Kantor and A. S. Solodovnikov, *Hypercomplex Numbers: An Elementary Introduction to Algebras*, Springer-Verlag, New York, Berlin, Heidelberg, 1989.

[4] N. N. Bogolubov, A. A. Logunov, A. I. Oksak, and I. Todorov, "General principles of quantum field theory," *Mathematical Physics and Applied Mathematics*, vol. 10, 1990.

[5] K. A. Iskakova and R. F. Akhmaltdinov, "Modeling of the crystal structure growth process of GaAs," *Applied Physics A: Materials Science and Processing*, vol. 109, no. 4, pp. 857–864, 2012.

[6] K. A. Iskakova, R. Akhmaltdinov, and A. Amanova, "About the energy levels of GaAs," *Journal of Physics: Conference Series*, vol. 510, p. 012038, 2014.

[7] K. A. Iskakova, R. Akhmaltdinov, and A. Amanova, "Nanoscience and Nanotechnology Letters," vol. 11, no. 5, pp. 621–629, 2019.

[8] K. Iskakova and R. Akhmaltdinov, "Nickel oxide nanoparticles on the surface of the gallium arsenide nanocluster structure," *Nano Energy*, vol. 8, no. 2, pp. 201–204, 2019.

[9] K. A. Iskakova, R. Akhmaltdinov, and B. Aliyev, "Interspheral space and properties of mono- and divalent metals with FCC and BCC structures," *Journal of Computational and Theoretical Nanoscience*, vol. 15, no. 4, pp. 1384–1394, 2018.

[10] K. Iskakova, R. Akhmaltdinov, and O. Mamyrbayev, "Production of thin copper oxide films and its electronic density," *AIMS Materials Science*, vol. 6, no. 3, pp. 454–463.

[11] K. A. Iskakova and R. Akhmaltdinov, "Modeling and calculation of the algorithm structure of compound Semiconductor-Type A^3B^5," *Applied Mechanics and Materials*, vol. 110-116, no. 7, pp. 2854–2858, 2011.

[12] T. R. Tulenbergenov, A. Z. Miniyazov, I. A. Sokolov, and G. K. Kayyrdy, "The role of a simulation stand with a plasma-beam installation in studies of plasma-surface interaction," *Bulletin of the NNC RK–2019*, vol. 4, pp. 51–58, 2017.

[13] V. A. Lisovskiy and S. D. Yakovin, *Experimental investigation of DC gas breakdown in argon*, Kharkov state university, scientific center of physical technologies, Ukraine, 1999.

[14] Y. H. Akhmadeev, Y. F. Ivanov, N. N. Koval, I. V. Lopatin, and P. M. Schanin, *Nitriding of commercially pure VT1-0 titanium and VT6 alloy in low pressure discharges*, Institute Of High Current Electronics SB RAS, Russia, 2011.

[15] R. Hoffmann, *Solids and Surface: A Chemist's View on Bonding in Extended Structures*, VCH Publishers, New York, 1988.

[16] S. Gražulis, D. Chateigner, R. T. Downs et al., "Crystallography open database – an open-access collection of crystal structures," *Journal of Applied Crystallography*, vol. 42, no. 4, pp. 726–729, 2009.

[17] XRD analysis of irradiated surface of tungsten samples, protocol dated 14.10.16, No. 12-230-02/861, IAE RSE NNC RK, Kurchatov 071100, Kazakhstan.

[18] Act of SEM-EDS analysis and microhardness measurement of tunsten samples after nitriding at PPD, act dated 17.10.2016, No. 12-230-20/865, IAE RSE NNC RK, Kurchatov, 071100, Kazakhstan.

[19] D. Bimberg, M. Grundmann, and N. N. Ledentsov, *Quantum Dot Heterostructures*, Wiley, Chichester, 1998.

[20] C. Y. Chang and F. Kai, *In GaAs High Speed Devices*, Wiley, New York, 1994.

[21] J. Cheon, Y.-w. Jun, and S.-M. Lee, "Architecture of Nanocrystal Building Blocks," in *Nanoparticles: Building Blocks for Nanotechnology (Chap 2)*, V. Rotello, Ed., pp. 53–87, Kluwer Academic, 2004.

[22] J. Nishizawa and T. Kurabayashi, "On the Reaction Mechanism of GaAs MOCVD," *Journal of the Electrochemical Society*, vol. 130, no. 2, pp. 413–417, 1983.

[23] A. Kallenbach, R. Dux, J. C. Fuchs et al., "Divertor power load feedback with nitrogen seeding in ASDEX Upgrade," *Plasma Physics and Controlled Fusion*, vol. 52, no. 5, p. 055002, 2010.

[24] A. Kallenbach, M. Balden, R. Dux et al., "Plasma surface interactions in impurity seeded plasmas," *Journal of Nuclear Materials*, vol. 415, no. 1, pp. S19–S26, 2011.

[25] K. Schmid, A. Manhard, C. Linsmeier et al., "Interaction of nitrogen plasmas with tungsten," *Nuclear Fusion*, vol. 50, no. 2, p. 025006, 2010.

[26] K. Dobes, P. Naderer, N. Lachaud, C. Eisenmenger-Sittner, and F. Aumayr, "Sputtering of tungsten by N+ and N2+ ions: investigations of molecular effects," *Physica Scripta*, vol. T145, p. 014017, 2011.

[27] Stand of simulation tests in support of studies in tokamak KTM (SII-KTM), final report, 85-3-021-129, Part 1, MEPhI (2005).